PII: Bonding and Densification

Outline:

- Solid state sintering (SSS) Models and Densification

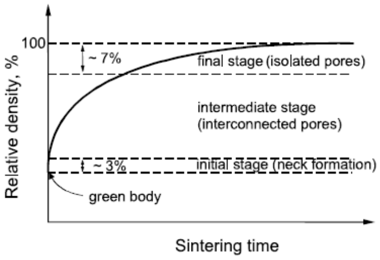

  - Models and kinetics
  - Effects of processing variables:

    particle size, temperature,
    external pressure, atmosphere
    (entrapped gases)

- Liquid phase sintering (LPS) Models and Densification
  - Validity of three stage models
  - Role of liquid in densification
  - Densification kinetics (effects of processing variables)

KAIST, S-J L. Kang

Chap. Solid State Sintering

Microstructure of a powder compact

Simplification of powder compact
as close-packed mono-size spherical particles

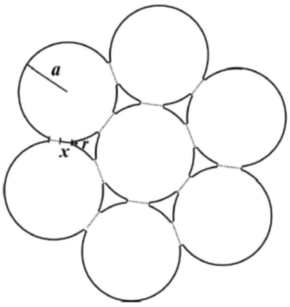

Bordia *et al. J. Am. Ceram. Soc.* **100,** 2315 (2017).

Representation with two particles:
Two Particle Model
for analysis of contact formation
and shrinkage
(Initial stage sintering)

Close-packed compact of
mono-sized particles
for analysis of densification
(Intermediate and
Final stage sintering)

Porosity:
Open (interconnected, apparent)
Closed (isolated)

KAIST, S-J L. Kang

Initial Stage Sintering

Qn: What is the driving force for neck growth and shrinkage?
(shape of pores)
Mechanisms?, Kinetics?

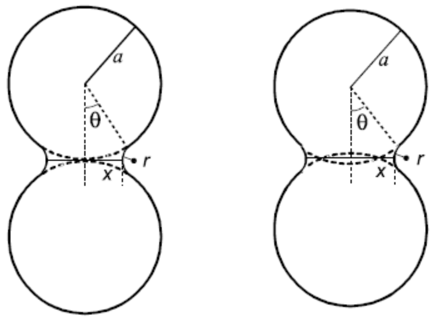

without shrinkage | with shrinkage

bonding only | bonding and densification

- Material flux = *f*(driving force)
  = *f*(neck geometry)

Without shrinkage	With shrinkage
$r \approx \frac{x^2}{2a}$	$r \approx \frac{x^2}{4a}$
$A \approx 2\pi x \cdot 2r = \frac{2\pi x^3}{a}$	$A \approx \frac{\pi x^3}{a}$
$V = \int A dx = \frac{\pi x^4}{2a}$	$V \approx \left(\pi x^2 \cdot 2r\right)/2 = \frac{\pi x^4}{4a}$

(For a >> x >> r ; acceptable for x < 0.3a)

KAIST, S-J L. Kang

Driving force in the two-particle model

(i) ΔP (pressure)

(ii)Vacancy conc. difference

(iii)Vapor pressure difference (solubility difference)

Sintering

Curved interface → pressure difference
(geometry of powder compacts) solubility difference parallel processes
- Interfacial energy vapor pressure difference
- <thermodynamics> (Δ(γA)) <kinetics> (geometry and σ)

Sintering Theory

KAIST, S-J L. Kang

Sintering Mechanisms

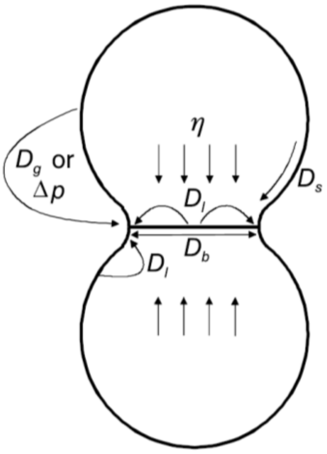

Two material sources :
grain boundary and surface
(with and without shrinkage)

Note: Material transport mechanisms and paths
(parallel processes)
Dominant mechanism = f(a, x, T)

Qn: Difference btw serial and parallel processes?
Controlling?, Dominant?

KAIST, S-J L. Kang

Role of Grain Boundary for Densification

Cu at 1075 ˚C

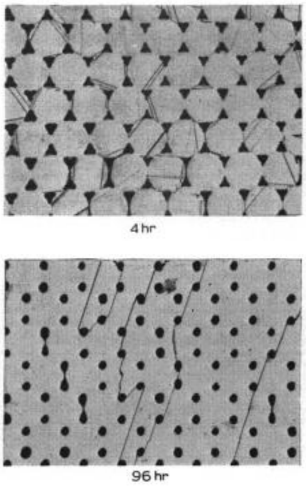

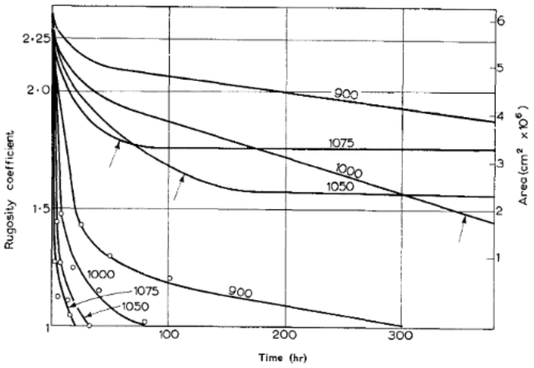

Void area and rugosity coefficient during isothermal sintering of 0·0128 cm dia. wires. Arrows indicate the approximate time when grain growth occurred.

Suppression of GG, in particular AGG

Alexander and Balluffi, *Acta Metall.,* **5**, 666 (1957).

KAIST, S-J L. Kang

Role of Grain Boundary for Densification

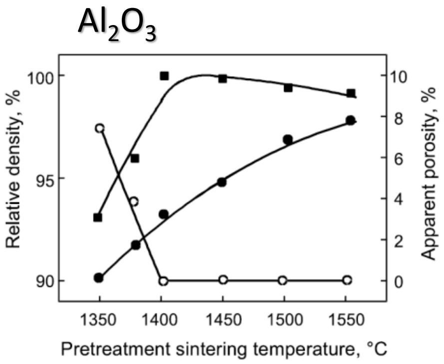

- The pores entrapped within grains cannot be eliminated even by hot isostatic pressing of a few thousand atm.

Figure 5.8. Effect of sintering temperature on the relative density (●) and the apparent porosity (○) before hot isostatic pressing, and on the relative density (■) after hot isostatic pressing.[55]

Kwon, *et al., J. Am. Ceram Soc.,* **70**, C69 (1987).

KAIST, S-J L. Kang

Sintering Mechanisms

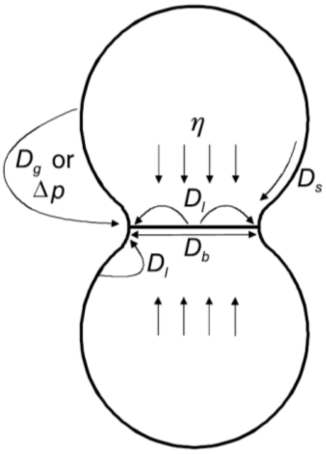

Two material sources :
grain boundary and surface
(with and without shrinkage)

Note: Material transport mechanisms and paths
(parallel processes)
Dominant mechanism = f(a, x, T)

Qn: Difference btw serial and parallel processes?
Controlling?, Dominant?

KAIST, S-J L. Kang

Sintering Kinetics

Lattice diffusion from grain boundary to neck

cf : diffusional creep of polycrystalline material under a stress gradient

(Nabarro-Herring Creep)

$$\frac{dV}{dt} = JAV_m = \frac{D}{RT}\nabla\sigma \cdot AV_m$$

J : Atom flux; *A* : Neck Area; V_m: Molar volume

Neck growth

$$\frac{dV}{dt} = JAV_m$$

$$\frac{\pi x^3}{a}\frac{dx}{dt} = \frac{D_l}{RT}\nabla\sigma \cdot A \cdot V_m$$

$$\approx \frac{D_l}{RT}\left(\frac{\gamma_s}{r}\frac{1}{x}\right)\frac{\pi x^3}{a}V_m$$

$$\therefore x^4 = \frac{16 D_l \gamma_s V_m a}{RT}t,$$

Shrinkage

$$\frac{\Delta l}{l} = \frac{r}{a} = \frac{x^2}{4a^2} = \left(\frac{D_l \gamma_s V_m}{RTa^3}\right)^{1/2} t^{1/2}$$

Grain Boundary diffusion from g-b to neck

(Coble Creep)

Neck growth

$$\therefore x^6 = \frac{48 D_b \delta_b \gamma_s V_m a^2}{RT}t,$$

Shrinkage

$$\frac{\Delta l}{l} = \frac{r}{a} = \left(\frac{3 D_b \delta_b \gamma_s V_m}{4RTa^4}\right)^{1/3} t^{1/3}$$

KAIST, S-J L. Kang

Summary of kinetic equations for various mechanisms of initial stage sintering

Sintering Mechanism	Neck Growth	Shrinkage	Scale exponent α
1. Lattice diffusion from grain-boundary to neck	$x^4 = \frac{16 D_l \gamma_s V_m a}{RT}t \equiv C_l D_l at$	$\frac{\Delta l}{l} = \left(\frac{D_l \gamma_s V_m}{RTa^3}\right)^{1/2} t^{1/2}$	3
2. Grain-boundary diffusion from grain-boundary to neck	$x^6 = \frac{48 D_b \delta_b \gamma_s V_m a^2}{RT}t \equiv C_b D_b \delta_b a^2 t$	$\frac{\Delta l}{l} = \left(\frac{3 D_b \delta_b \gamma_s V_m}{4RTa^4}\right)^{1/3} t^{1/3}$	4
3. Viscous flow	$x^2 = \frac{4\gamma_s a}{\eta}t \equiv C_{vf}\frac{1}{\eta}at$	$\frac{\Delta l}{l} = \frac{3\gamma_s}{8\eta a}t$	1
4. Surface diffusion from particle surface to neck	$x^7 = \frac{56 D_s \delta_s \gamma_s V_m a^3}{RT}t \equiv C_s D_s \delta_s a^3 t$		4
5. Lattice diffusion from particle surface to neck	$x^5 = \frac{20 D_l \gamma_s V_m a^2}{RT}t \equiv C_l' D_l a^2 t$		3
6. Gas phase transport			
6-1. Evaporation-condensation from particle surface to neck	$x^3 = \sqrt{\frac{18}{\pi}}\frac{p_\infty \gamma_s}{d^2}\left(\frac{M}{RT}\right)^{3/2} at \equiv C_{e/c}\, p_\infty at$		2
6-2. Gas diffusion from particle surface to neck	$x^5 = 20 p_\infty D_g \gamma_s \left(\frac{V_m}{RT}\right)^2 a^2 t \equiv C_g\, p_\infty D_g a^2 t$		3

D_l, D_b, D_s and D_g: the lattice, grain boundary, surface and gas diffusion coefficients, respectively;
δ_b and δ_s: the diffusion thicknesses of the grain boundary and of the surface diffusion; η: viscosity;
d: the material density; M: the molar weight of the material; C_i: a constant for mechanism i;
R: the gas constant (8.314 J/K·mol); T: the absolute temperature.

Assumptions: No GG, φ = 180°, Local equilibrium

KAIST, S-J L. Kang

Usefulness and limitations of initial stage sintering theory (kinetic eqs)

$$\left(\frac{x}{a}\right)^n = F(T)\left(\frac{1}{a^{n-m}}\right)t$$

Qn: Determination of
sintering mechanism?

(i) Estimation of the effect of processing variables

particle size, temperature, time

(ii) Estimation of the relative contribution of different processes

eg) lattice diffusion vs. surface diffusion

The relative contribution depends on x, a, and T.

→ **Sintering Diagram**

Simultaneous (parallel) processes

(Observed kinetics is the sum of the
kinetics of all different processes)

KAIST, S-J L. Kang

Sintering Diagram

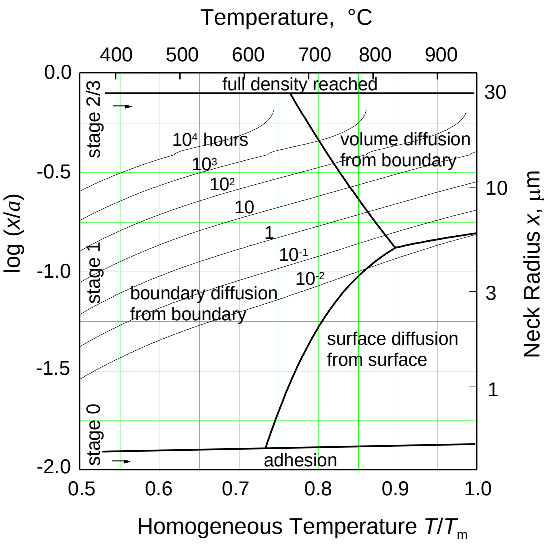

Ag (a = 38μm)

$$\left(\frac{dx}{dt}\right)_t = \sum_{i=1}\left(\frac{dx}{dt}\right)_i$$

i : mechanism i

With No Grain Growth

M. F. Ashby, *Acta Metall.*, **22**, 275 (1974)

KAIST, S-J L. Kang

Effect of Sintering Variables

$$\left(\frac{x}{a}\right)^n = F(T)\left(\frac{1}{a^{n-m}}\right)t$$

- Scale (size)

Scaling law for systems with similar figures, and the same and invariable sintering mechanism

C. Herring, *J. Appl. Phys.* **21**, 301 (1950)

t = V/JAVm **t**: time required to get the same microstructural change

JAVm = the rate of material transport,

V scales as L^3, A scales as L^2, a scales as L,

eg) volume diffusion mechanism

$$t = \frac{V}{JAV_m} = \frac{L^3}{((D_l/RT)(2\gamma_s/L)(1/L))L^2V_m} \propto L^3$$

Qn: viscous flow?
evaporation-condensation?

$$\boldsymbol{t_2 = (\lambda)^{\alpha} t_1}$$

λ : scale
α : scale exponent

$\alpha = n\text{-}m$

KAIST, S-J L. Kang

Effect of Sintering Variables

$$\left(\frac{x}{a}\right)^n = F(T)\left(\frac{1}{a^{n-m}}\right)t$$

- Temperature

for Diffusion and Viscous flow

$$\left(\frac{x}{a}\right)^n \propto \left(\frac{D_l}{T}\right)a^{m-n}t$$

Qn: vapor phase transport?

- Pressure

$\sigma_t = \gamma/r + P_{appl.}$

Qn: effect of scale?

- Composition

in case of vacancy diffusion?

Qn: effect of dopants?

KAIST, S-J L. Kang

Inter. and Final Stage Sintering

Qn: How can we simplify the pore geometry?
(microstructure of the compact)

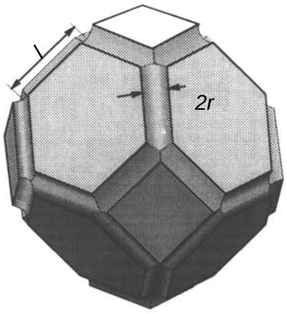

Intermediate stage model

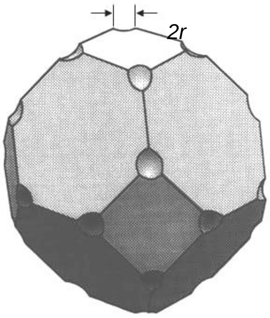

Final stage model

- A tetrakaidecahedral grain has 14 planes (grain boundaries) with 8 hexagons and 6 squares, 36 3-grain edges, and 24 4-grain corners

KAIST, S-J L. Kang

Sintering Models and Kinetics

Early Model

Intermediate Stage

Final Stage Model

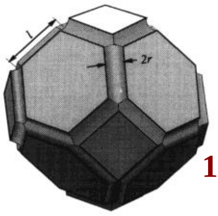

14 disks

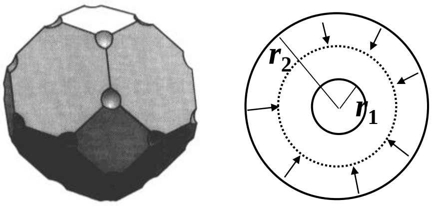

24 isolated pores

Disk Model for ***D_l* and *D_b***

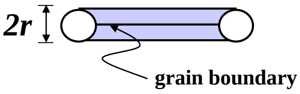

Concentric Sphere Model for ***D_l***

$$J_{total} = const. = 4\pi r^2 \frac{D_l}{RT}\frac{d\sigma}{dr} \Big/ pore$$

material flux

$$J_{atom} = 4\pi \frac{D}{RT}\Delta\sigma$$

R. L. Coble, *J. Appl. Phys.*, **32**, 789 (1961)

KAIST, S-J L. Kang

Sintering Models and Kinetics

Developed Model

Consideration of diffusion area for densification: $\frac{dV}{dt}=JAV_m$

Lattice Diffusion:
surface area of the pore

$$\frac{d\rho}{dt}=\frac{441D_l\gamma_s V_m}{RTG^3}(1-\rho)^{1/3}$$

$$cf: \frac{288D_l\gamma_s V_m}{RTG^3}$$

(Coble's Eq.)

Grain Boundary Diffusion:
grain boundary length at the pore surface

$$\frac{d\rho}{dt}=\frac{733D_b\delta_b\gamma_s V_m}{RTG^4}$$

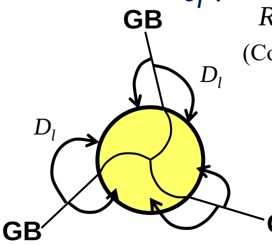

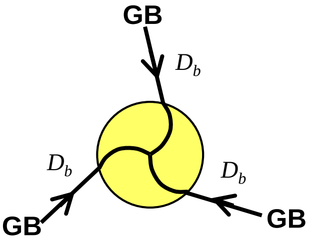

Kang and Jung, *Acta Mater.,* **52**, 4373 (2004)

Kinetic eqs at Intermediate and Final Stage Sintering

Densification Mechanism		Densification Rate	Scale Exponent α
Intermediate stage	1. Lattice diffusion from grain boundary to pore	$\frac{d\rho}{dt}\approx\frac{290D_l\gamma_s V_m}{G^3RT}$	3
	2. Grain boundary diffusion from grain boundary to pore	$\frac{d\rho}{d\rho}\approx\frac{230D_b\delta_b\gamma_s V_m}{G^4RT(1-\rho)^{1/2}}$	4
Final Stage	1. Lattice diffusion from grain boundary to pore	$\frac{d\rho}{dt}\approx\frac{440D_l\gamma_s V_m}{G^3RT}(1-\rho)^{1/3}$	3
	2. Grain boundary diffusion from grain boundary to pore	$\frac{d\rho}{dt}\approx\frac{730D_b\delta_b\gamma_s V_m}{G^4RT}$	4

Final Stage Sintering Diagram

Effect of grain size (Al_2O_3)

Grain growth was taken into account (Eq. (11.20))

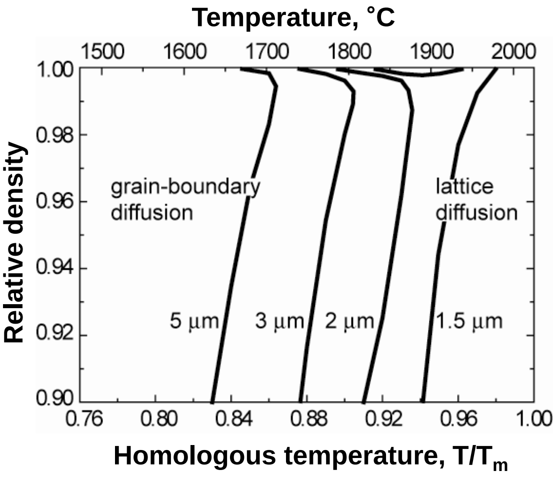

Qn: At a constant T, why does the dominant mechanism change?

$D_l \rightarrow D_b \rightarrow D_l$

Kang and Jung, *Acta Mater.,* **52**, 4373 (2004)

KAIST, S-J L. Kang

Pressure-Assisted Sintering

Hot pressing, Hot isostatic pressing, Gas pressure sintering

- Simultaneous use of heat and pressure –
  Densification enhancement, no effect on GG
- Driving force:
  Neck area (initial) and relative density (intermediate and final) dependent. $P_1^* = \frac{4\pi a^2}{\pi x^2 Z\rho} P_{appl.} + \frac{\gamma_s}{r}$ $P_2^* \approx P_{appl.} + \frac{2\gamma_s}{r}$
- Densification Models:
  (i) Plastic yielding
  $P_1^* \geq \sigma_i \approx 3\sigma_Y$ $P_2^* \geq \frac{2}{3}\sigma_Y \ln\left(\frac{1}{1-\rho}\right)$
  (ii) Power law creep
  $\frac{d\rho}{dt} = f(\rho, \text{geo})\frac{x}{a}\dot{\varepsilon}_o\left(\frac{P_1^*}{3\sigma_o}\right)^n$ $\frac{d\rho}{dt} = f(\rho)\dot{\varepsilon}_o\left(\frac{3}{2n}\frac{P_2^*}{\sigma_o}\right)^n$
  (iii) Diffusion
  $\frac{d\rho}{dt} = f(\rho, \text{geo})\frac{(D_b\delta_b + rD_l)V_m}{RTa^3}P^*$

Note: scaling law

KAIST, S-J L. Kang

Change in Pore size during Sintering

Change in pore size is the results of

- Size reduction by densification
- Size increase by pore coalescence due to GG
- Effect of entrapped insoluble gases?

Qn: Pore growth by Ostwald ripening?
in insoluble atmosphere
in soluble atmosphere
in vacuum sintering

KAIST, S-J L. Kang

Entrapped Insoluble Gases and Densification

Practical case I

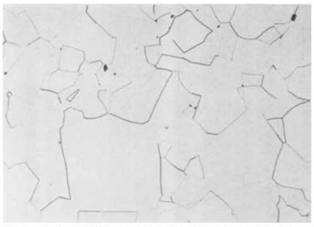

Fig. 3. Alumina containing magnesia fired in hydrogen for 21 hours at 1850°C and then for 23 hours at 1900°C; density, 3.97 g per cm³ (×255.)

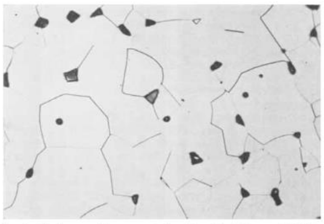

Fig. 4. Alumina containing magnesia fired in air for 21 hours at 1850°C, for 23 hours at 1900°C, and refired in hydrogen for 18 hours at 1900°C; density, 3.95 g per cm³. (×255.)

Coble*, J. Am. Ceram. Soc.,* **45**, 123 (1962).

Practical case II

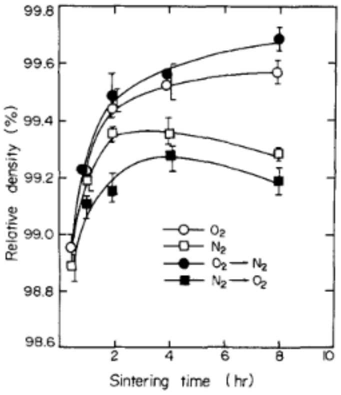

Fig. 2. Variation of sintered density with sintering time of 1000-ppm-MgO-doped alumina sintered at 1600°C in O_2, N_2, $O_2 \rightarrow N_2$, and $N_2 \rightarrow O_2$. The atmosphere change was done after 30 min of sintering.

Qn: Why dedensification (bloating)?

Paek *et al., J. Am. Ceram. Soc.,* **71**, C380 (2006).

KAIST, S-J L. Kang

Exercise:

Insoluble gases and volume expansion of pores with grain growth

Growth from size G to 2G of cube-shaped grains with pores at their corners

With the grain growth, 8 pores (r_1) coalesce into one pore (r_2)

Assuming $P_{ext} = 0$, $P_1V_1 = P_2V_2$

$$P_1V_1 = 8\times(4/3)\pi r_1^{3\times}(2\gamma/r_1) = P_2V_2 = (4/3)\pi r_2^{3\times}(2\gamma/r_2)$$

$$\therefore r_2 = \sqrt{8}r_1$$

$$(4/3)\pi r_2^3 = 8\sqrt{8}\pi r_1^3$$

A volume increase by √8 times,

in general, by √n times

KAIST, S-J L. Kang

Entrapped Insoluble Gases and Densification

Maximum attainable density (Limiting density)

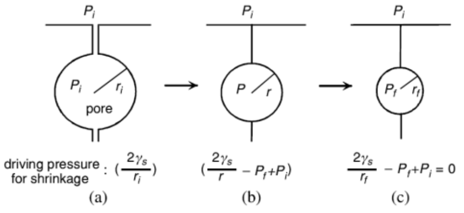

Figure 5.4. Schematic of pore shrinkage during sintering:[40] (a) just before the isolation of the pore, (b) shrinkage stage, and (c) final state.

$$P_i\left[\left(r_i/r_f\right)^3-1\right] = 2\gamma_s/r_f$$

Limiting density = f(ri, Pi, γs)

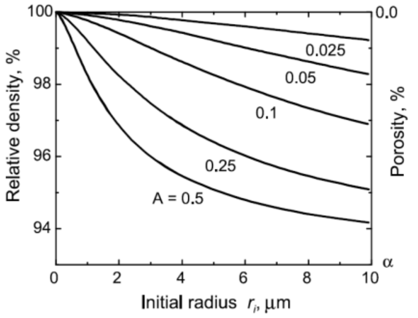

Figure 5.5. Maximum attainable density versus r_i, with an initial porosity of α% ($A = P_i/2\gamma_s$ µm^{-1}).[40] The ordinate is scaled by assuming an initial density of 93% of the theoretical value.

$P_i/(2\gamma/r_i) = 0.05$ for P_i is 1atm, γ is 1J/m^2 and r_i is 1µm

Benefits of fine powder:

(i) lower entrapped gas effect

(ii) higher densification kinetics

Qn: Effect of external pressure?

Qn: Effect of GG (pore coalescence)

Kang and Yoon, *J. Eu. Ceram. Soc.,* **5**, 135 (1989).

KAIST, S-J L. Kang

Particle Size Distribution and Densification

Monosize powder or powder with a size distribution?

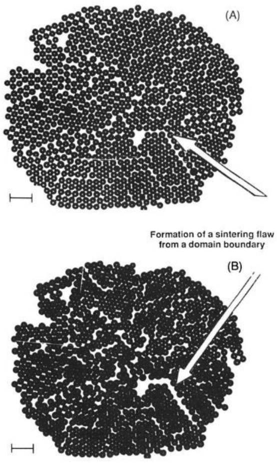

Effect of sintering on a two dimensional layer of monosized 140 μm glass spheres: (A) befor and (B) after sintering at 1273 K for 4h; bar = 500 μm.

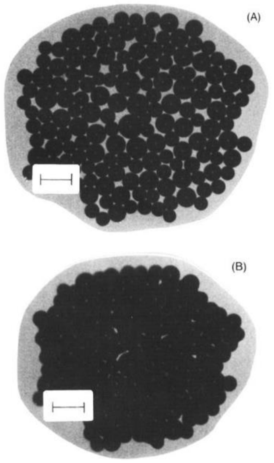

Effect of sintering on a bimodal mixture of glass spheres (60% 80 μm, 40% 100 μm): (A) before and (B) after sintering at 1273 K for 4h; bar = 200 μm.

Liniger and Raj, *J. Am. Ceram. Soc.*, **70**, 843 (1987)

KAIST, S-J L. Kang

Particle Size Distribution and Densification

Unimodal or bi-/multi-modal distribution?

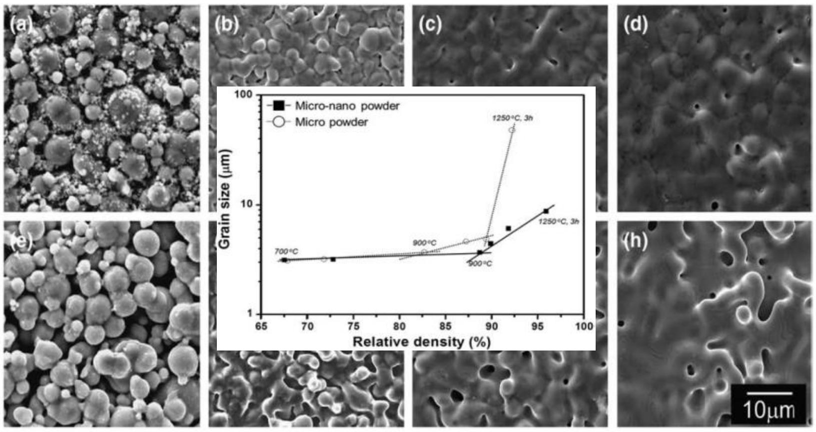

Fig. 6. SEM micrographs of the heat-up sintered parts using (a)–(d) Fe micro–nanopowder and (e)–(h) micropowder under different sintering temperatures (×7000): (a, e) 700 °C, (b, f) 900 °C, (c, g) 1100 °C and (d, h) 1250 °C.

Choi *et al., Powder Tech.*, **253**, 591 (2012).

KAIST, S-J L. Kang

Chap. Liquid Phase Sintering

Example of Densification Curves

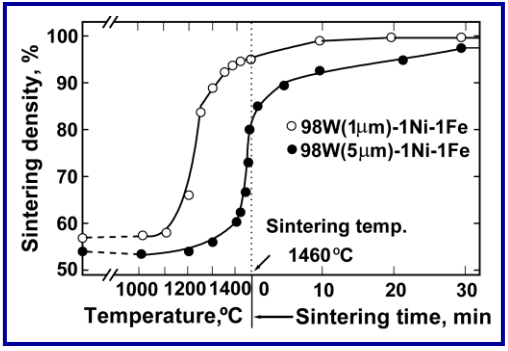

Park et al., *Metall Trans. A,* **20,** 837 (1989)

Qn: Differences btw.
LPS and SSS?

Role of liquid?
Mass transport?
Equili. microstructure?

Phenomena occurring during LPS:

- Alloying and skeleton formation, if any, during heating
- Liquid formation/flow and particle rearrangement, if any
- Dissolution and precipitation of solid – densification and grain growth
- Liquid filling of pores - densification

KAIST, S-J L. Kang

Flow (redistribution) of Liquid

due to uneven capillary pressure

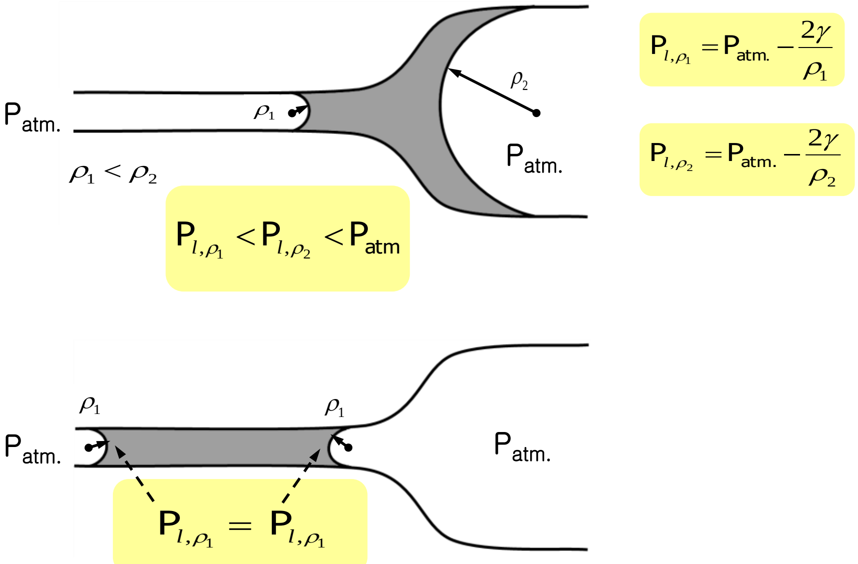

$$P_{l,\rho_1} = P_{atm.} - \frac{2\gamma}{\rho_1}$$

$$P_{l,\rho_2} = P_{atm.} - \frac{2\gamma}{\rho_2}$$

$$P_{l,\rho_1} < P_{l,\rho_2} < P_{atm}$$

$$P_{l,\rho_1} = P_{l,\rho_1}$$

KAIST, S-J L. Kang

Particle Rearrangement

due to the capillary action of liquid

- Wettability of liquid (wetting angle) is critical for liquid redistribution and particle rearrangement.
- For a low wetting angle, liquid can penetrate btw. particles.
- Particle rearrangement can take place if there is no bonding btw. particles or if the dihedral angle is 0^{o}.
- The contribution of particle rearrangement to densification is insignificant because of local densification as well as pore growth.

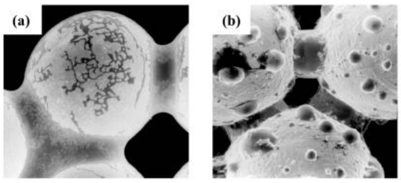

Figure 14.5. Distribution of liquid Cu between W spheres (~200 µm diameter) for a wetting angle θ of (a) 8° and (b) 85°.[2]

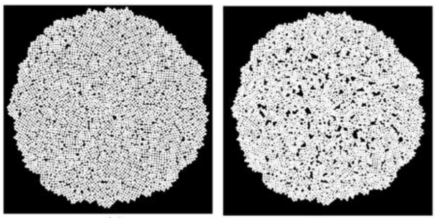

Simulated microstructural evolution of a two-dimensional particle array with holding time for liquid viscosity of 1 mPa · s

Huppmann and Riegger, *Acta Metall.*, **23**, 965 (1975)

Lee, et al., *Metals Mater.* **5**, 197 (1999)

KAIST, S-J L. Kang

Microstructure at Early Stage of LPS

Skeleton formation, if any, during heating

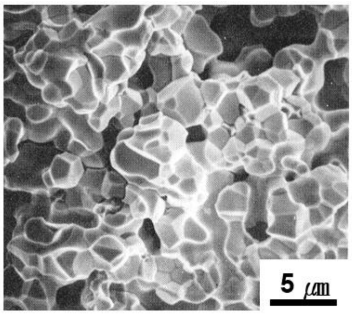

Fracture surface of W (5 µm)-Ni-Fe sample heated up to 1450°C.

Microstructure right after liquid formation

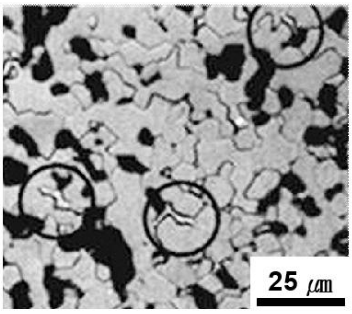

W (5 µm)-Ni-Fe sample sintered at 1460°C for 0 min.

Park et al., *Metall Trans. A,* **20,** 837 (1989)

Microstructural Characteristics at early stage of LPS

- Liquid: a continuous phase
- Solid grains: interconnected and mostly surrounded by liquid
- Pores of irregular shapes

KAIST, S-J L. Kang

Example of Microstructural Evolution during LPS

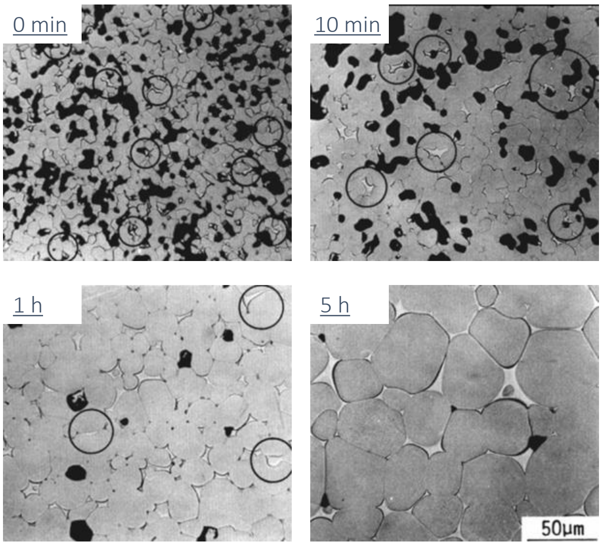

98W (5µm) -1Ni-1Fe
1460 °C

Park et al.,
Metall. Trans. A, **20**, 837 (1989)

KAIST, S-J L. Kang

Densification Mechanisms

Contact Flattening

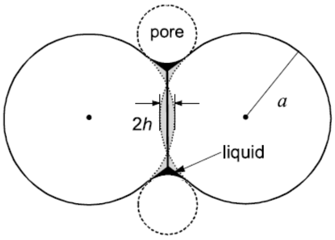

Kingery's two-particle model of liquid phase sintering.

- Transport of atoms from the contact area of grains to the off-contact area through a thin liquid film btw grains. (This process is called contact flattening, of which the result is an increase of contact area.) (Kingery, *J. Appl. Phys.*, **30**, 301 (1959))
- ***The liquid acts as a diffusion medium of atoms.***

Kingery's eq. for diffusion control: $\frac{\Delta l}{l_0} = \frac{h}{a} \approx \frac{1}{3}\frac{\Delta V}{V} = \left(\frac{6k_1\delta_l D C_\infty \gamma V_m}{RT}\right)^{1/3} a^{-4/3} t^{1/3}$

- For an idealized system with micron-sized spherical grains, liquid volume fraction of 5%, and dihedral angle of zero degrees, a theoretical calculation suggested that several per cent of shrinkage can be achieved by contact flattening in less than a minute. (Lee and Kang, *Z. Metallkde*, **92**, 669 (2001))
- In real systems, such a fast densification has never been observed.
- In real systems, in particular for those with non-zero dihedral angle, the contribution of contact flattening to densification is negligible.

KAIST, S-J L. Kang

Densification Mechanisms

Pore Filling *Mass flow of liquid*

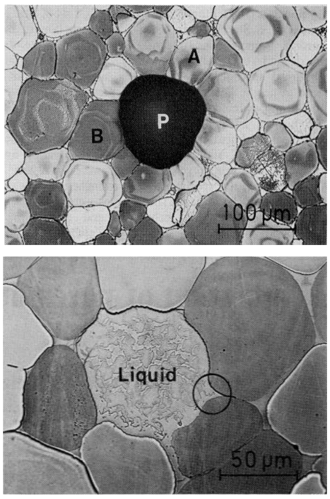

Mo - Ni

Kang et al., *Powder Metall.*, **27**, 97 (1984)

In a real system

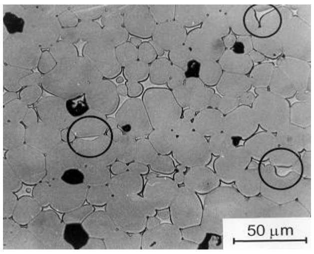

W - Ni - Fe

Park et al., *Metall. Trans. A*, **20**, 837 (1989)

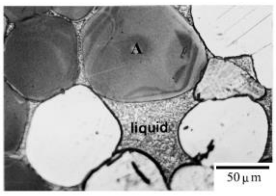

KAIST, S-J L. Kang

Microstructural Evolution for two different mech.

Qn: Driving force for densification? (Consider equilibrium shape of grains.)

(a) Contact Flattening (Kingery, 1959)

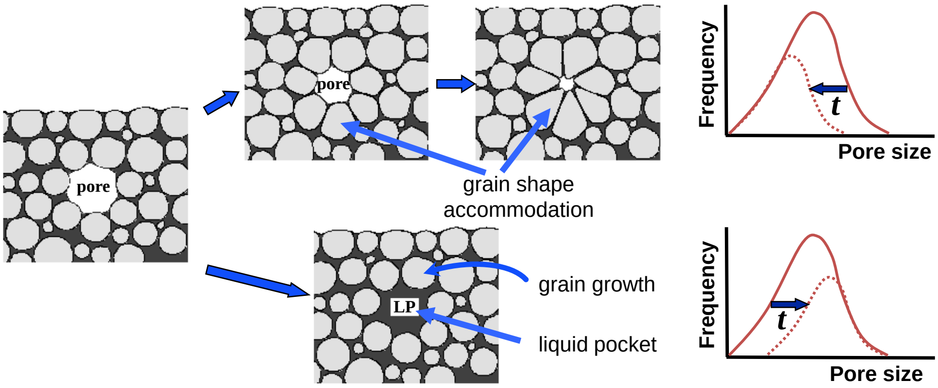

(b) Pore filling (Kwon & Yoon, 1980; Park et al. 1989; Kang et al. 1991)

Kingery, *J. Appl. Phys.*, **30**, 301, 1959

Kwon and Yoon, in *Sintering Processes*, G. C. Kuczinski (ed.), Plenum Press, New York, 208, 1980
Park, et al., *Metall. Trans. A*, **20**, 837 (1989)
Kang et al., *J. Am. Ceram. Soc.*, **74**, 425 (1991)

KAIST, S-J L. Kang

Microstructural Evolution during LPS

Change in Pore Intercept Distribution

98W (5µm) -1Ni-1Fe
1460 °C

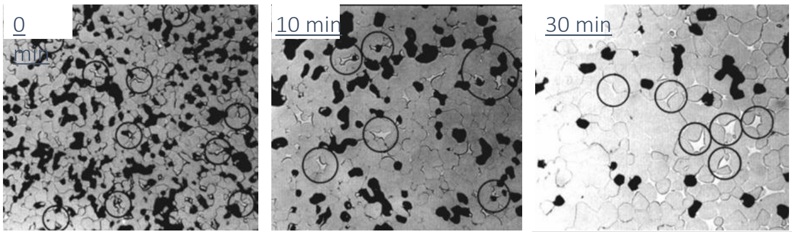

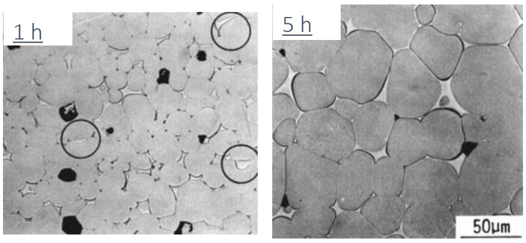

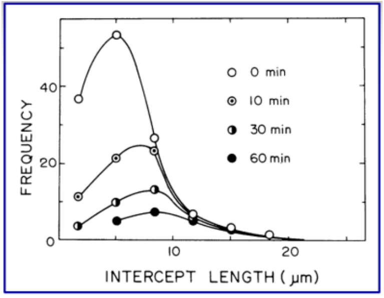

Park et al., *Metall. Trans. A*, **20**, 837 (1989)

KAIST, S-J L. Kang

Surface Microstructures

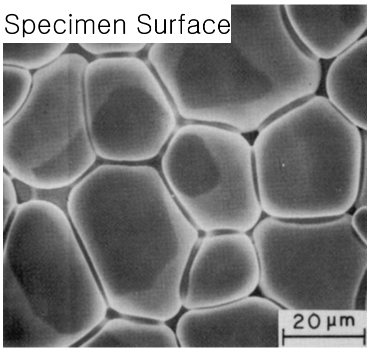

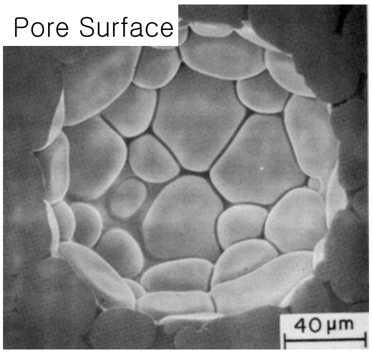

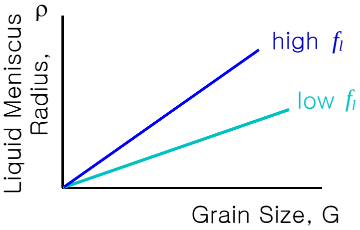

Park et al., *Metall. Trans. A*, **17A**, 325 (1989)

KAIST, S-J L. Kang

Pore Filling Mechanism

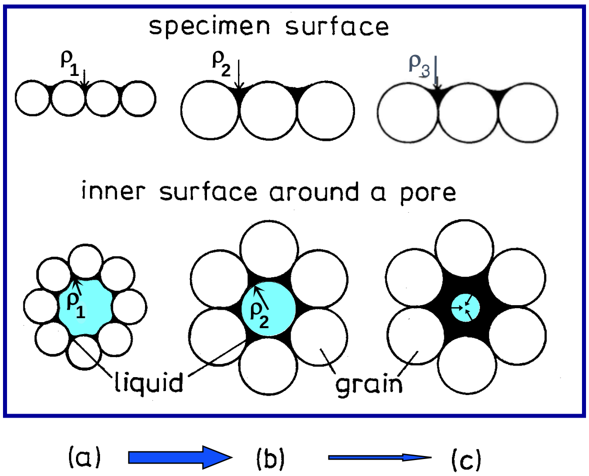

Grain Growth

$P_1^{surf} = P_1^{pore}$ $P_2^{surf} = P_2^{pore}$ $P_3^{surf} > P_2^{pore}$

$$P_l^{surf} = P_{atm.} - \frac{2\gamma}{\rho_s}$$

$$P_l^{pore} = P_{atm.} - \frac{2\gamma}{\rho_p}$$

- ***Critical Moment :*** ***Complete Wetting of Pore Surface***

Kang et al., *J. Am. Ceram. Soc.*, **72**, 1166-69 (1989)

KAIST, S-J L. Kang

Relationship btw Grain Size and Pore Filling

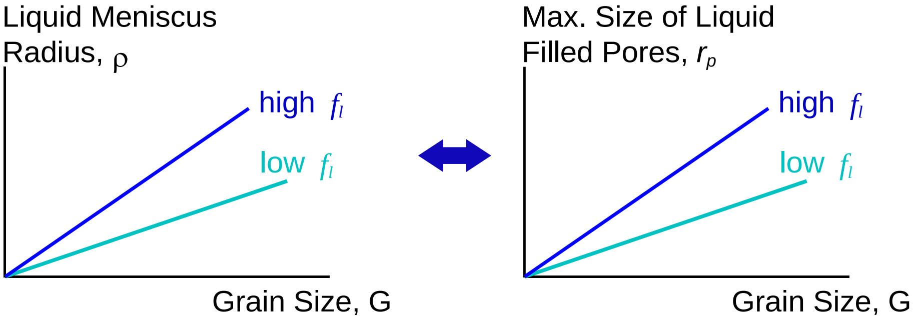

$\rho \propto G$ $\rho \leftrightarrow r_p$ $r_p \propto G$

Liquid filling of pores in temporal sequence

KAIST, S-J L. Kang

Pore Filling Model

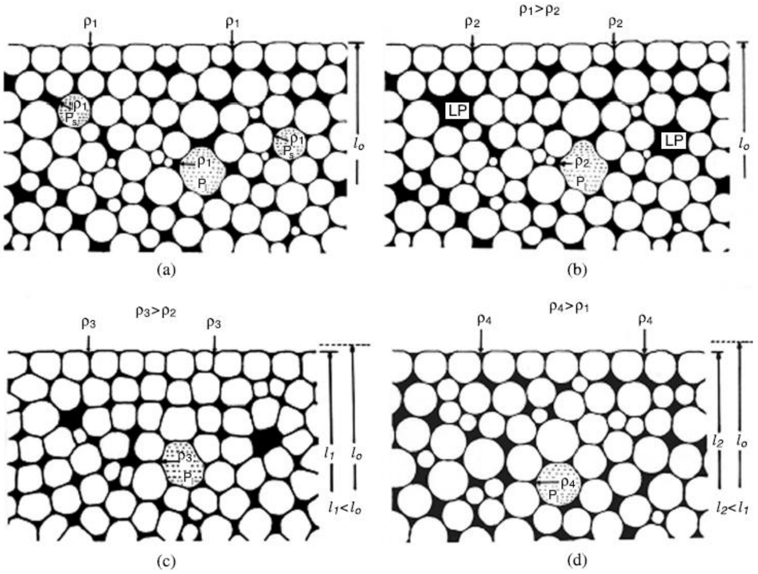

Kang et al., *J. Am. Ceram. Soc.*, **74**, 425-27 (1991)

KAIST, S-J L. Kang

Pore Filling Theory

Calculation scheme

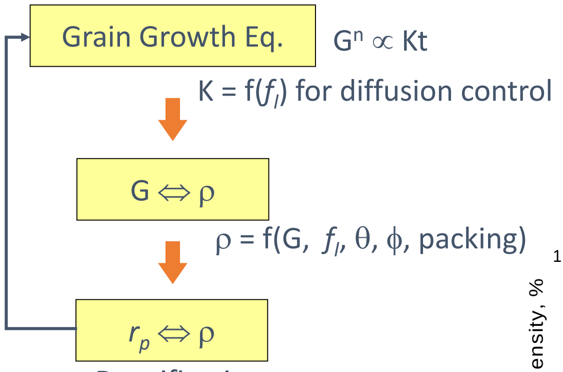

Grain Growth Eq. $G^n \propto Kt$

$K = f(f_l)$ for diffusion control

$G \Leftrightarrow \rho$

$\rho = f(G,\ f_l,\ \theta,\ \phi,\ \text{packing})$

$r_p \Leftrightarrow \rho$

Densification

*Effective liquid volume fraction

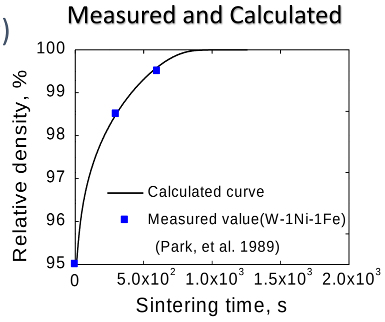

Lee and Kang, *Acta Mater.*, **46**, 3191 (1998)

KAIST, S-J L. Kang

Pore Filling Theory

Experimental Support

Effect of Initial WC particle size

Measured densification curves

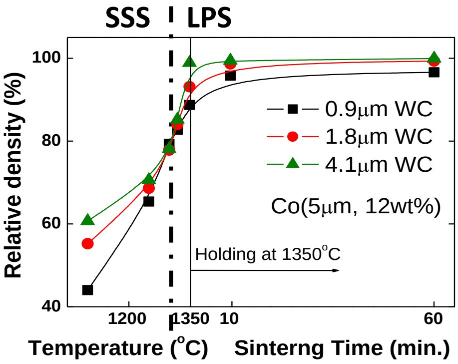

Caculated curves with data points

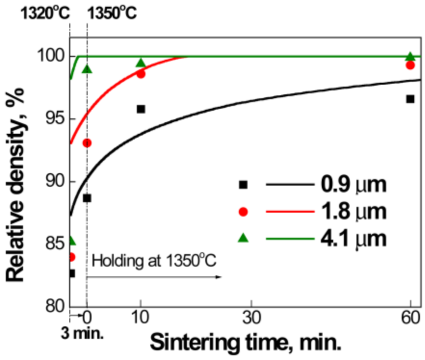

In LPS **faster densification** in samples with **larger WC grains**.

Kim et al., *J. Am. Ceram. Soc.*, **88**, 2106 (2005)

KAIST, S-J L. Kang

Pore Filling Theory

Experimental Support

Effect of Abnormal Grain Growth

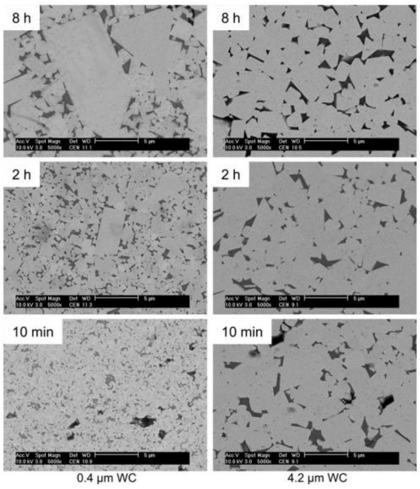

95WC-5Co

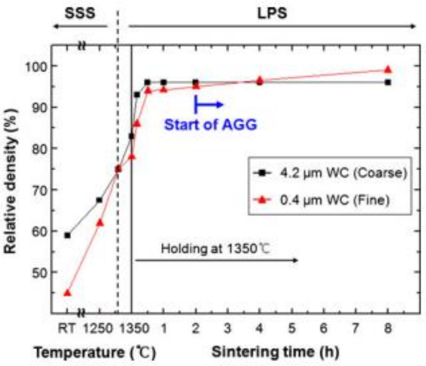

Full densification in samples
with **abnormal growth of WC grains**.

Yang, et al, *J. Mater. Sci.*, **47**, 7056 (2012)

KAIST, S-J L. Kang

Effect of Scale

- Particle size ($T_{m,s} \rangle T_{m,l}$)

Powder with high T_m : r_s
Powder with low T_m : r_l

Time needed for densification

	$2r_l$	r_l	$1/2\ r_l$
$2r_s$	$8t_o$	$< t_o$	$< 1/8\ t_o$
r_s	$> 8t_o$	t_o	$< 1/8\ t_o$
$1/2\ r_s$	$> 8t_o$	$> t_o$	$1/8\ t_o$

-Diffusion-controlled grain growth
($G^3 \propto Kt$)

-Initial pore size ← r_l

Dominant effect of the size of particles with low T_m

➡ Beneficial effects of using
i) Low-T_m-powder of small size, and
ii) High-T_m-powder of large size
] r_s/r_l ratio ↑
This conclusion is particularly true when $r_l > r_s$

KAIST, S-J L. Kang

Effect of Pore and Liquid Volume Fraction

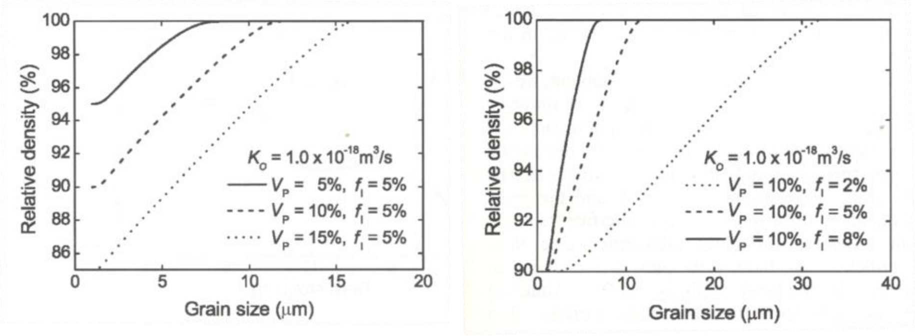

$$\frac{d\rho}{dG} \approx const.$$

$$\frac{d\rho}{dG} \propto f_l^{1.3}$$

Lee and Kang, *Z. Metallkunde*, **96**, 141-47 (2005)

KAIST, S-J L. Kang

Effect of Wetting and Dihedral Angle

Effect of Wetting Angle

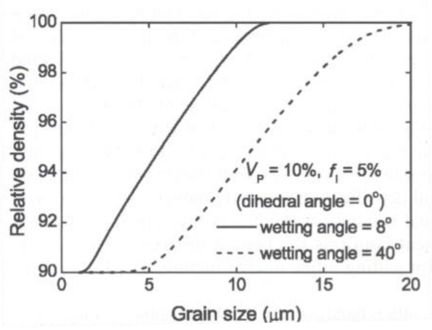

Effect of Dihedral Angle

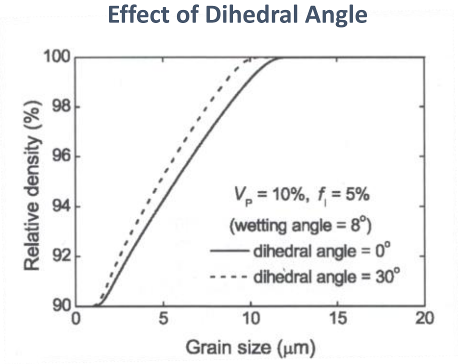

Lee and Kang, *Z. Metallkunde*, **96**, 141-47 (2005)

KAIST, S-J L. Kang

Effect of Entrapped Gases

82Fe-18Cu

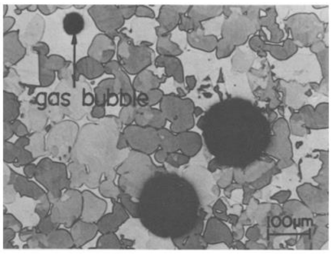

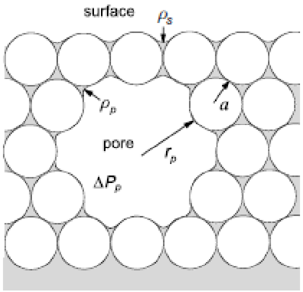

$$\frac{a(\Delta P_p)}{a(0)} = \frac{\rho_s(\Delta P_p)}{\rho_s(0)} = \frac{\rho_s(\Delta P_p)}{r_p}$$

$$\Delta P_p = 2\gamma\left(\frac{1}{\rho_p} - \frac{1}{\rho_s}\right)$$

$$\frac{a(\Delta P_p)}{a(0)} = \frac{1}{1 - \frac{1}{2} r_p \Delta P_p / \gamma_l}$$

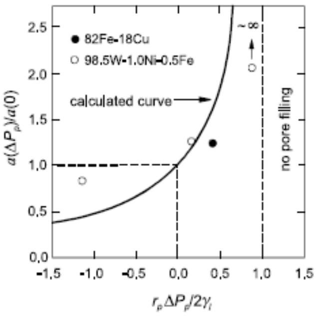

Cho, et al., *Metall. Trans. A*, **17A**, 2175 (1986)

Kang et al., in *Horizons of Powder Metallurgy*, Kaysser and Huppman (eds), Verlag Schmid GmbH, Freiburg, 1214 (1986)

KAIST, S-J L. Kang

Densification and Grain Growth

Solid-state sintering (SSS)

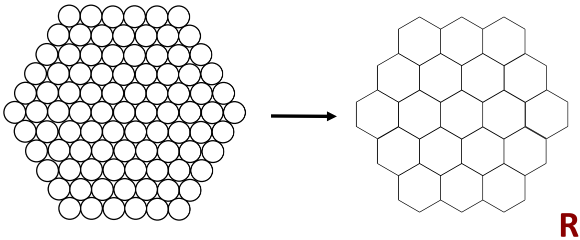

Role of Liquid in
Densification
(shape accommodation) &
Grain growth

Liquid-phase sintering (LPS)

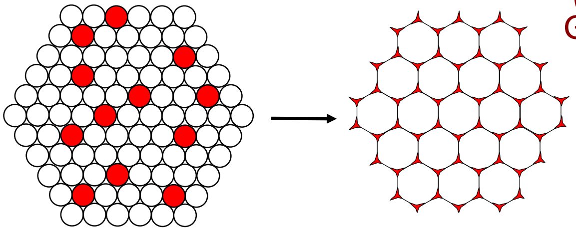

"Liquid phase sintering: Fundamentals" in "*Encyclopedia of Materials: Technical Ceramics and Glasses,*" A. Leriche and F. Cambier (eds), Elsevier (2020).

Exercises:

- Relative contribution of D_l and D_b with T and a
- Why faster densification in LPS than in SSS
- Gas pressure sintering in SSS and in LPS

Qn: Full Densification?

S.-J. L. Kang, *Materials*, 13, 3578 (2020)